Electronic Supplementary Information (ESI)

Bilayer Phosphorene Under High Pressure: *In Situ* Raman Spectroscopy

Meysam Akhtar[a,b], Congyan Zhang[a], Manthila Rajapaksa[a], Md Rajib Khan Musa[a], Ming Yu[a], Gamini Sumanasekera[a,b], Jacek B. Jasinski[b*]

[a] *Department of Physics and Astronomy, University of Louisville, Louisville, KY, 40292, USA*

[b] *Conn Center for Renewable Energy Research, University of Louisville, Louisville, KY, 40292, USA*

* Corresponding author: E-mail: jacek.jasinski@louisvill.edu, Phone: +1-502-852-6338

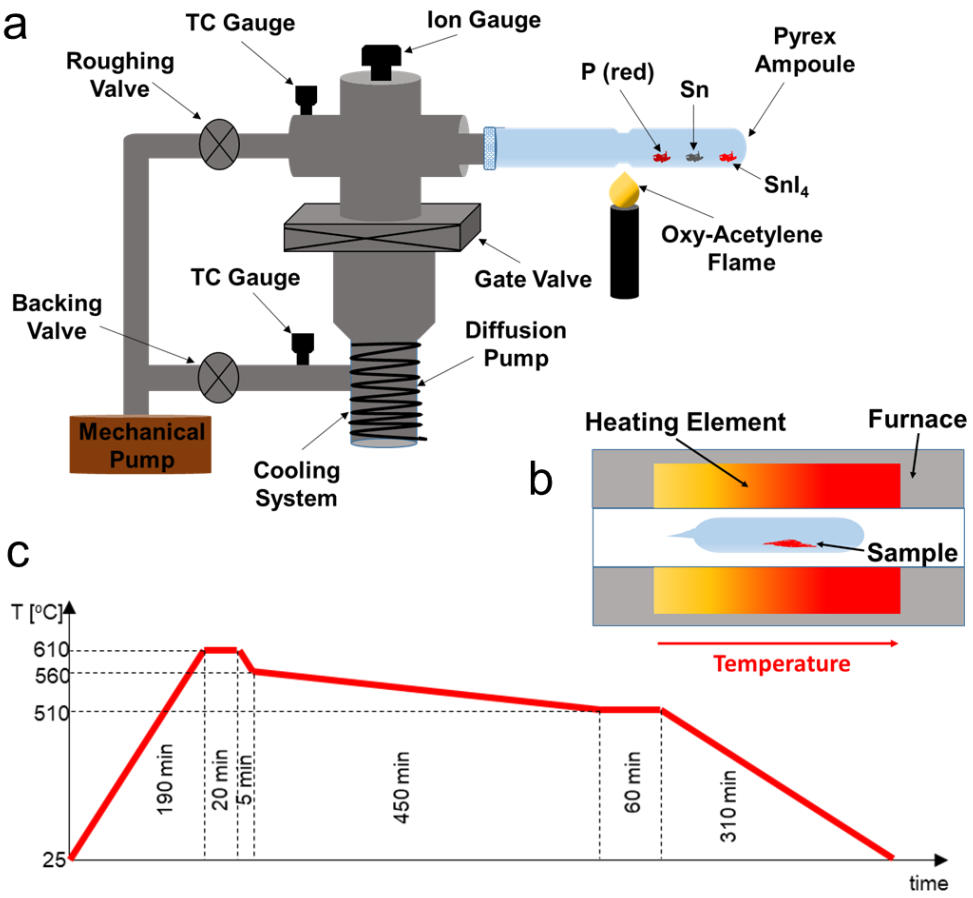

Fig. S1 Schematics of experimental setup for the short transport growth method of black phosphorous: (a) preparation of an evacuated quartz ampule containing the precursor materials, (b) synthesis of black phosphorous in a furnace (c) temporal temperature profile during the growth steps.

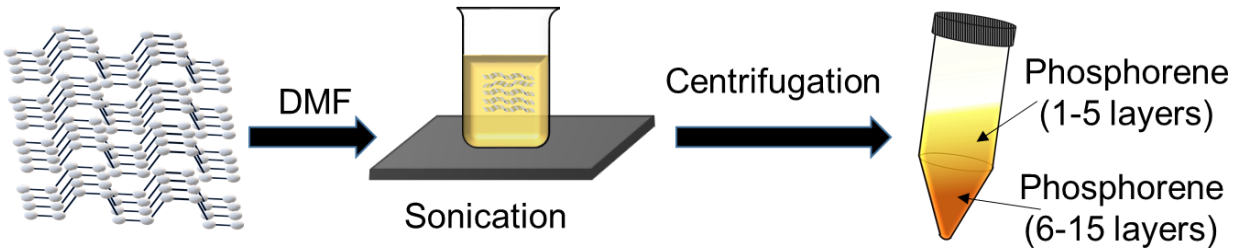

Fig. S2 A schematic showing liquid mechanical exfoliation and centrifugation of phosphorene samples.

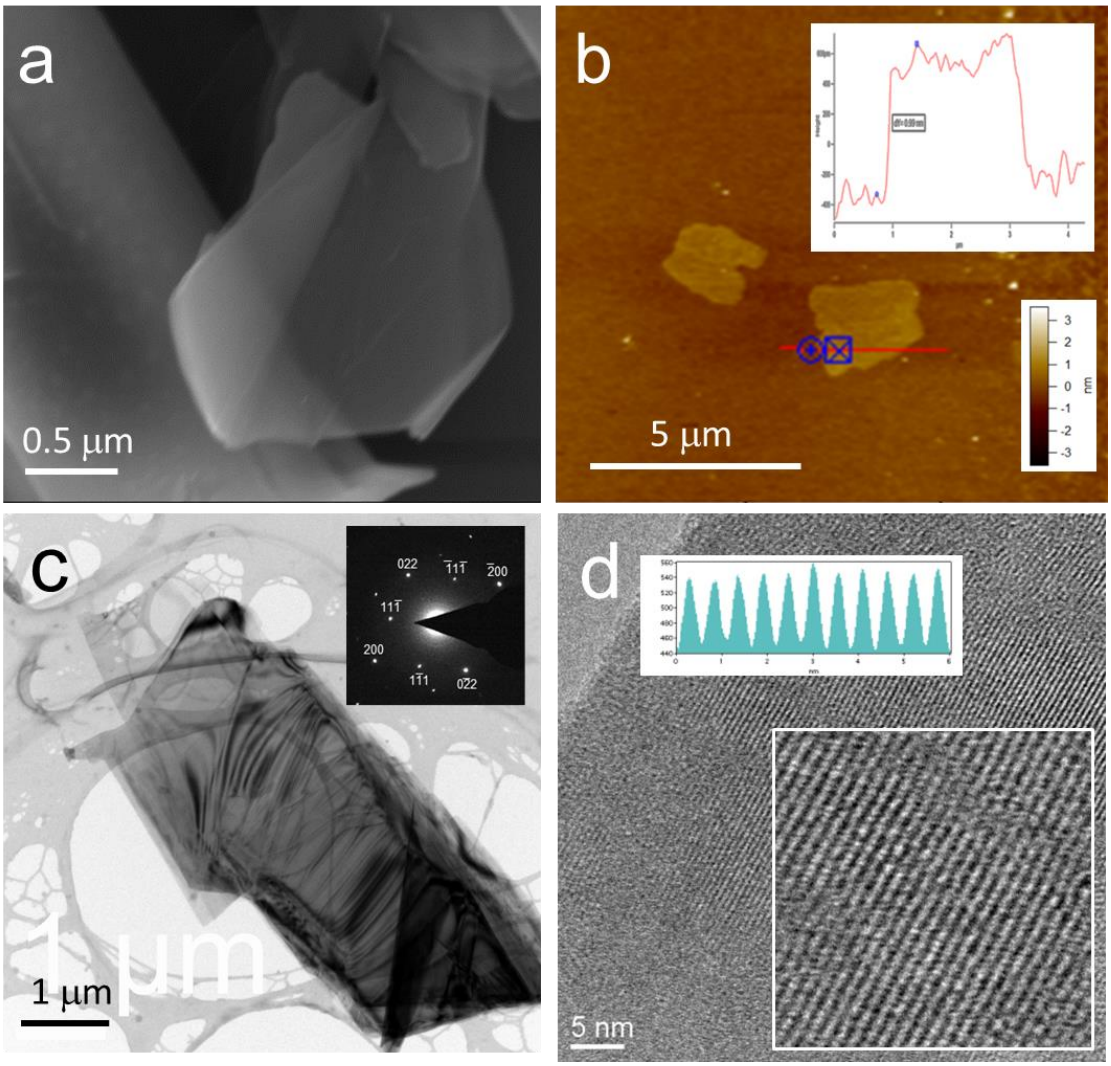

Fig. S3 Characterization of phosphorene samples: (a) SEM image of a few layer phosphorene flakes. (b) AFM image of two phosphorene flakes deposited on a Si substrate. The corresponding thickness profile measured from one of these flakes is included as an inset. (c) Low-magnification TEM image of a phosphorene flake deposited on a supporting holey carbon film. A single crystalline diffraction pattern is included as an inset. (d) High-resolution TEM (HRTEM) image of a phosphorene flake. A zoomed in section showing lattice fringes is included as one of insets. The corresponding intensity profile is shown above as a second inset.

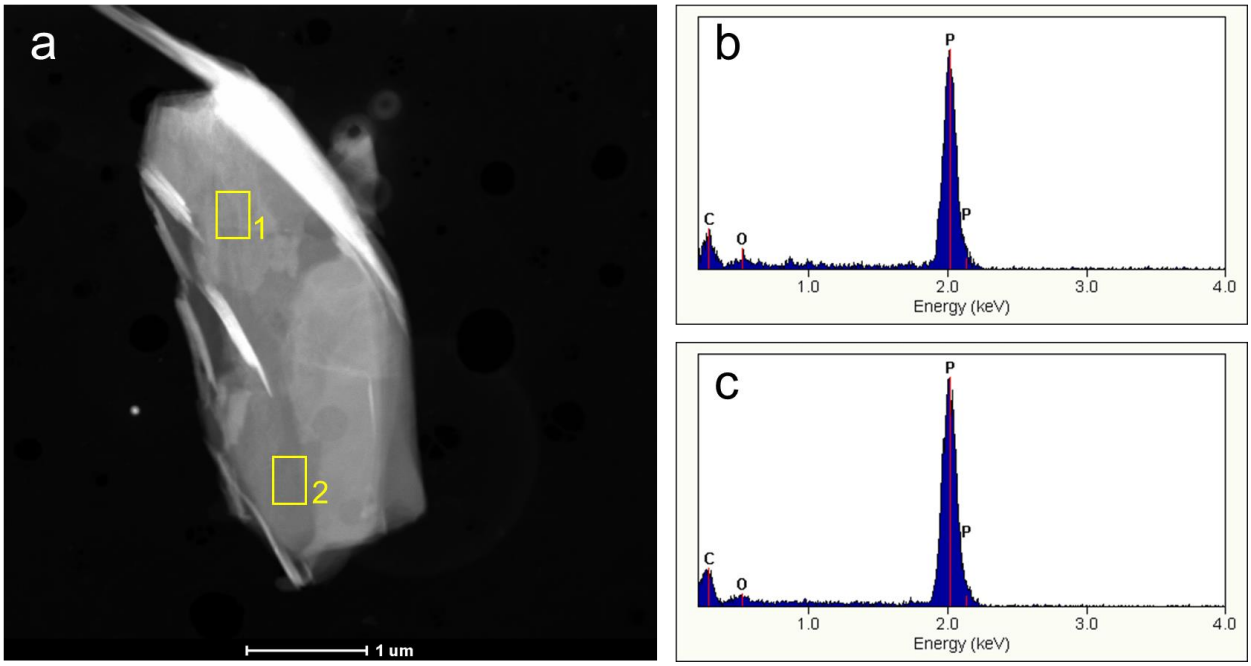

Fig. S4 EDS analysis of phoshorene: (a) STEM image of a single flake, (b) an (c) EDS spectra from regions 1 and 2 marked in (a).

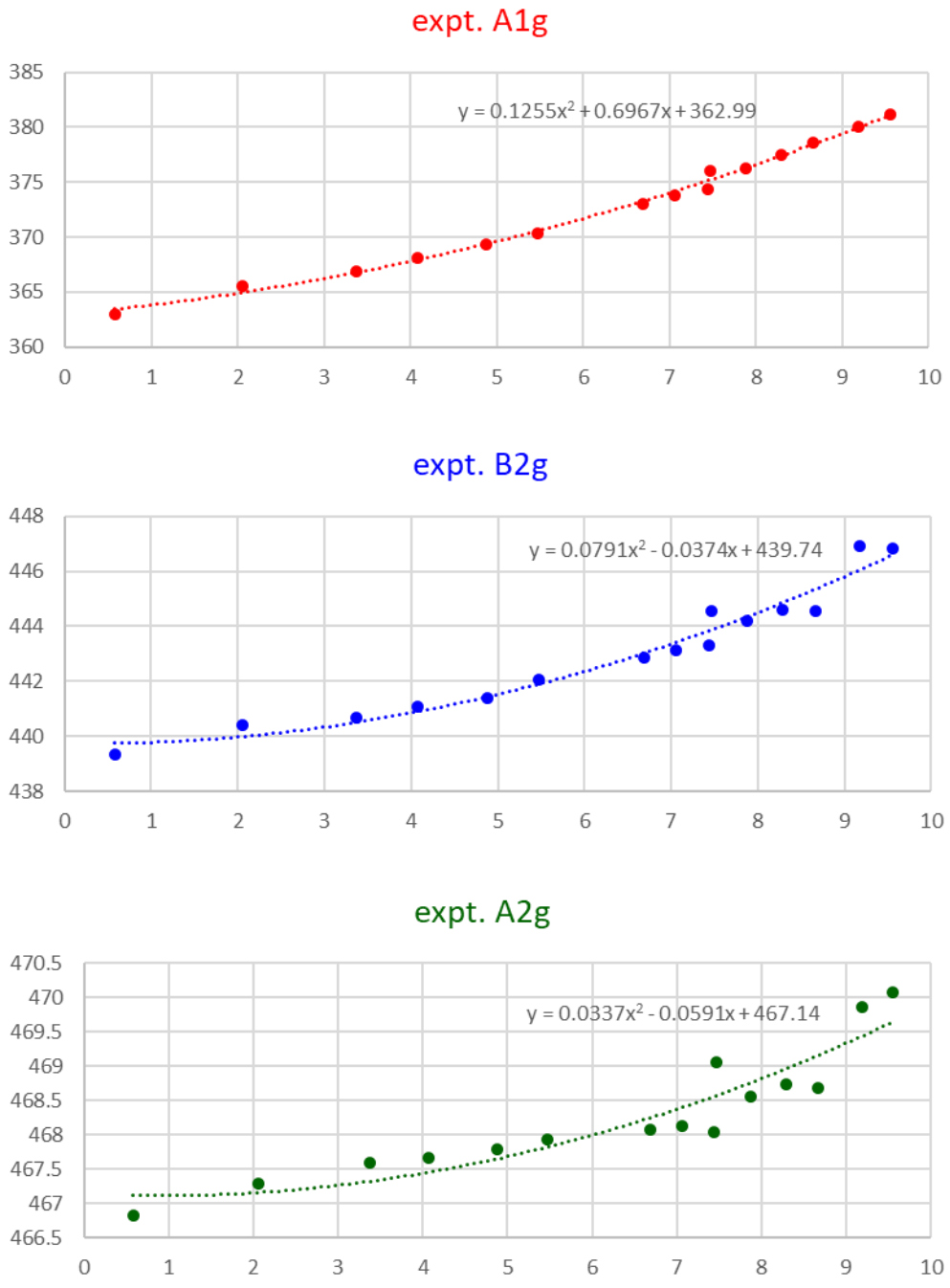

Fig. S5 The quadratic function fitting of experimental pressure dependence of the Raman shifts of the A1g, B2g, and A2g modes in bilayer phosphorene sample.

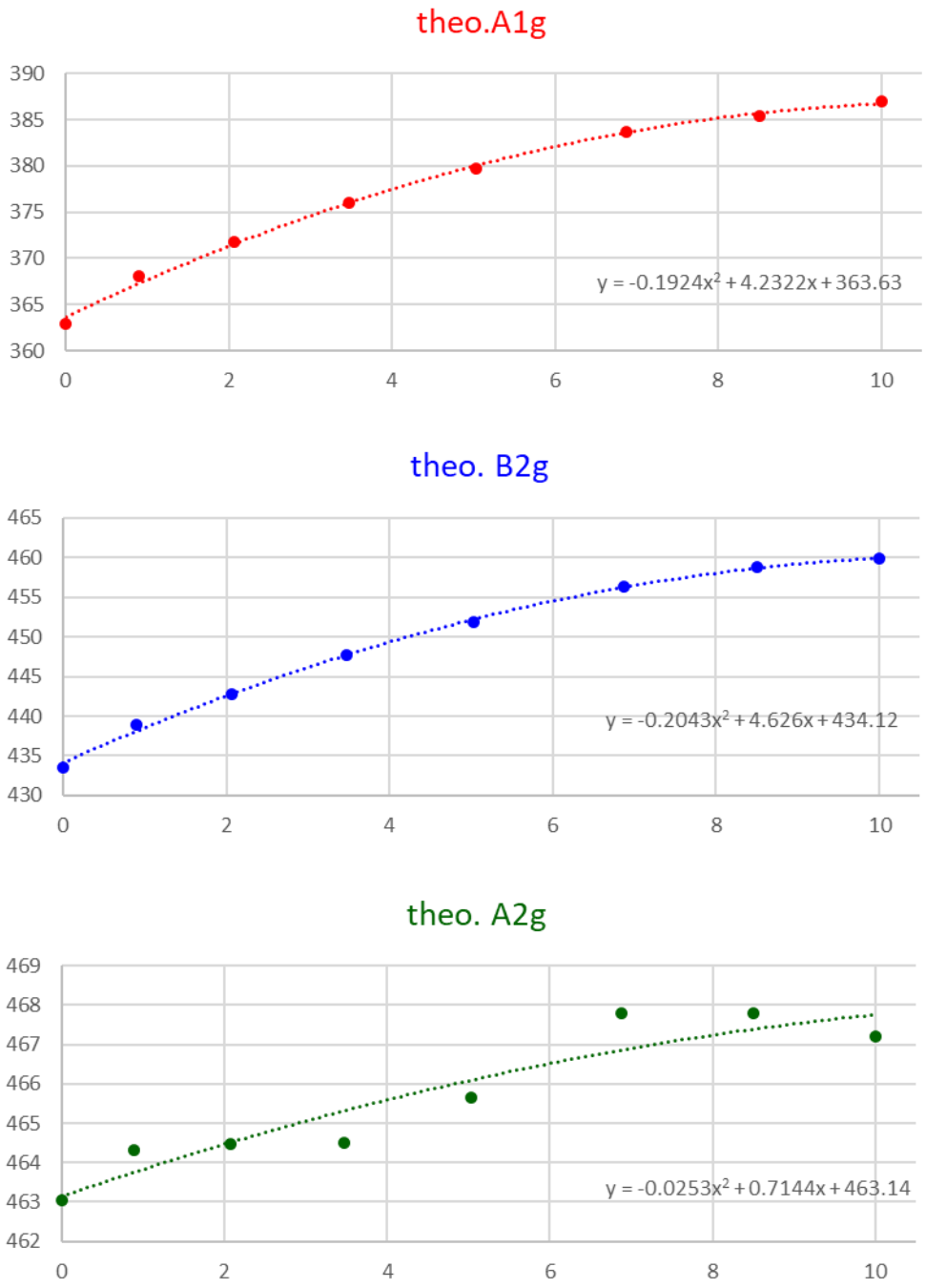

Fig. S6 The quadratic function fitting of theoretical pressure dependence of the Raman shifts of the A1g, B2g, and A2g modes in bulk black phosphorous.

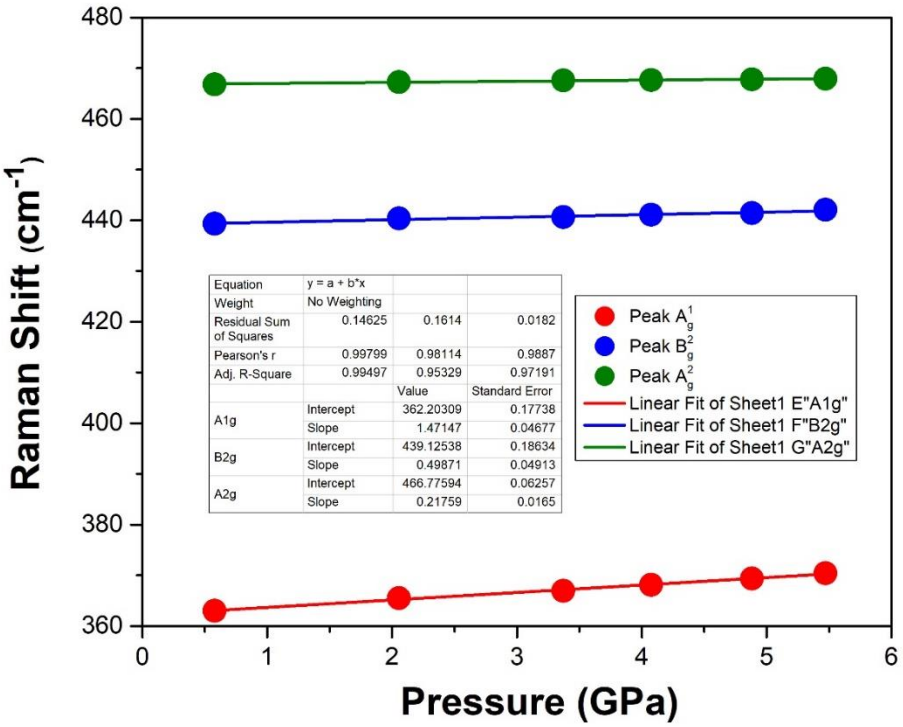

Equation	y = a + b*x		
Weight	No Weighting		
Residual Sum of Squares	0.14625	0.1614	0.0182
Pearson's r	0.99799	0.98114	0.9887
Adj. R-Square	0.99497	0.95329	0.97191
		Value	Standard Error
A1g	Intercept	362.20309	0.17738
	Slope	1.47147	0.04677
B2g	Intercept	439.12538	0.18634
	Slope	0.49871	0.04913
A2g	Intercept	466.77594	0.06257
	Slope	0.21759	0.0165

Fig. S7 The linear function fitting of the initial slopes of the Raman shifts all 3 main modes in bilayer phosphorene sample, for the pressures of up to 5 GPa.

Table S1 Raman shifts and pressure coefficients for the A1g, B2g, and A2g modes in bilayer phosphorene sample.

experimental data						
pressure	A1g	B2g	A2g	coefficient A1g	coefficient B2g	coefficient A2g
0.57762	363.001	439.3371	466.828	0.839141092	0.053979484	-0.020168412
2.056	365.483	440.4072	467.2865	1.2037096	0.2878592	0.0794744
3.37226	366.9241	440.6588	467.5896	1.528299316	0.496091532	0.168190324
4.07478	368.1258	441.0872	467.6623	1.701540748	0.607230196	0.215540172
4.88152	369.3751	441.4029	467.8	1.900482832	0.734856464	0.269914448
5.4721	370.3779	442.0499	467.9357	2.04611986	0.82828622	0.30971954
6.688	372.9731	442.845	468.0723	2.3459608	1.0206416	0.3916712
7.0547	373.7774	443.1099	468.1239	2.43638902	1.07865354	0.41638678
7.43684	374.3218	443.3008	468.0384	2.530624744	1.139108088	0.442143016
7.46386	376.0424	444.5701	469.0652	2.537287876	1.143382652	0.443964164
7.87688	376.2457	444.1839	468.568	2.639138608	1.208722416	0.471801712
8.2899	377.435	444.5975	468.7408	2.74098934	1.27406218	0.49963926
8.66432	378.5441	444.543	468.6771	2.833321312	1.333295424	0.524875168
9.18156	380.0889	446.9079	469.8557	2.960872696	1.415122792	0.559737144
9.55212	381.168	446.815	470.0687	3.052252792	1.473745384	0.584712888

Table S2 Raman shifts and pressure coefficients for the A1g, B2g, and A2g modes in bulk black phosphorous.

theoretical data						
pressure	A1g	B2g	A2g	coefficient A1g	coefficient B2g	coefficient A2g
0	362.8897	433.5526	463.0551	4.2322	4.626	0.7144
0.89289	368.0546	438.8729	464.3164	3.888794506	4.26170088	0.669219766
2.0679	371.83	442.829	464.464	3.43688566	3.7822968	0.60976426
3.47383	376.0206	447.6982	464.5179	2.896164982	3.20867736	0.538624202
5.03411	379.697	451.876	465.644	2.296081294	2.57208312	0.459674034
6.87837	383.7432	456.3677	467.803	1.586778898	1.81962504	0.366354478
8.5072	385.401	458.76	467.807	0.96033088	1.1550624	0.28393568
10.002	386.974	459.94	467.217	0.3854308	0.545184	0.2082988